Anatomic Moment

The Endolymphatic Duct and Sac

William W. M. Lo, David L. Daniels, Donald W. Chakeres, Fred H. Linthicum, Jr, John L. Ulmer, Leighton P. Mark, and Joel D. Swartz

The endolymphatic duct (ED) and the endolymphatic sac (ES) are the nonsensory components of the endolymph-filled, closed, membranous labyrinth. The ED leads from the utricular and saccular ducts within the vestibule through the vestibular aqueduct (VA) to the ES, which extends through the distal VA out the external aperture of the aqueduct (Fig 1) to terminate in the epidural space of the posterior cranial fossa. Thus, the ED-ES system consists of components both inside and outside the otic capsule connected by a narrow passageway through the capsule (1). In nomenclature, the osseous VA should be clearly distinguished from the membranous ED and ES, which it transmits. The VA is visible on computed tomography (CT), and the undilated ED and ES with their stroma on magnetic resonance (MR) imaging.

Traditionally, anatomic texts have depicted the ED-ES system as a single-lumen tubular structure, with a long thin ED ending in a short, blunt, pouchlike ES (2–4). In recent years, computer-aided reconstructions of histologic sections have revealed a system far different in appearance (5) (Figs 2 and 3). The ED is, in fact, a *short* single-lumen tubule, only about 2 mm in length (6), whereas the ES is a much larger and highly *complex* structure of interconnecting tubules, cisterns and crypts (5, 7, 8) (Fig 4). Variously described as shaped like a spindle, a paddle, a sail, or even a Christmas tree (5, 9–11) (Figs 2 and 3), the ES is highly variable in size (12) and quite irregular in outline, especially distally (13).

The ED forms from the confluence of the utricular and saccular ducts (7) (Fig 3). Its proximal, mildly fusiform segment, the sinus, lies in a groove on the posteromedial surface of the vestibule (14), while its major portion is contained within the short, slightly upwardly arched, horizontal segment of the VA (6, 15). After entering the VA, the sinus tapers to its intermediate segment within the horizontal segment of the VA, and then narrows at its isthmus within the isthmus of the VA (13). The mean diameters of the ED, 0.16×0.41 mm at the internal aperture of the VA and 0.09×0.20 mm at the isthmus, are below the resolution of present MR imagers (Fig 6A). The corresponding measurements of the VA, 0.32×0.72 and 0.18×0.31 mm, also challenge the resolution of current CT scanners.

Distal to the isthmus of the ED begins the ES, which flares considerably transversely but thickens only slightly in its sagittal dimension. The proximal, intraosseous portion of the sac, lying within the transversely widening, vertical segment of the VA, is covered posteriorly by a thin scale of bone, the operculum. The distal, extraosseous portion of the sac rests on a fovea on the posterior wall of the petrous bone, between layers of dura (13) (Figs 5C and 6A). The middle portion of the sac can lie in or out of the aqueduct depending on the length of the VA. The distal end of the sac overlaps the sigmoid sinus in as many as 40% of the cases (12) (Fig 2). The extraosseous portion of the sac varies widely from about 5 to 7 mm in width to about 10 to 15 mm in length (12, 13). Its intraosseous portion also varies widely in size depending on the size of the VA, which normally measures some 6 to 15 mm in length, 3 to 15 mm in width, and up to 1.4 mm in sagittal dimension of external aperture (15–17). Thus the normal ES is of sufficient size to be outlined by high-quality

From the Department of Radiology, St Vincent Medical Center, Los Angeles, Calif (W.W.M.L.), the Section of Neuroradiology, Department of Radiology, Medical College of Wisconsin, Milwaukee (D.L.D., J.L.U., L.P.M.), the Department of Radiology, Ohio State University, Columbus (D.W.C.), the House Ear Institute, Los Angeles (F.H.L.), and the Department of Radiology, Germantown Hospital and Medical Center, Philadelphia, Pa (J.D.S.)

Address reprint requests to William W. M. Lo, MD, 2131 W Third St, Los Angeles, CA 90057.

Index terms: Anatomic moments; Temporal bone, anatomy

AJNR 18:881–887, May 1997 0195-6108/97/1805–0881

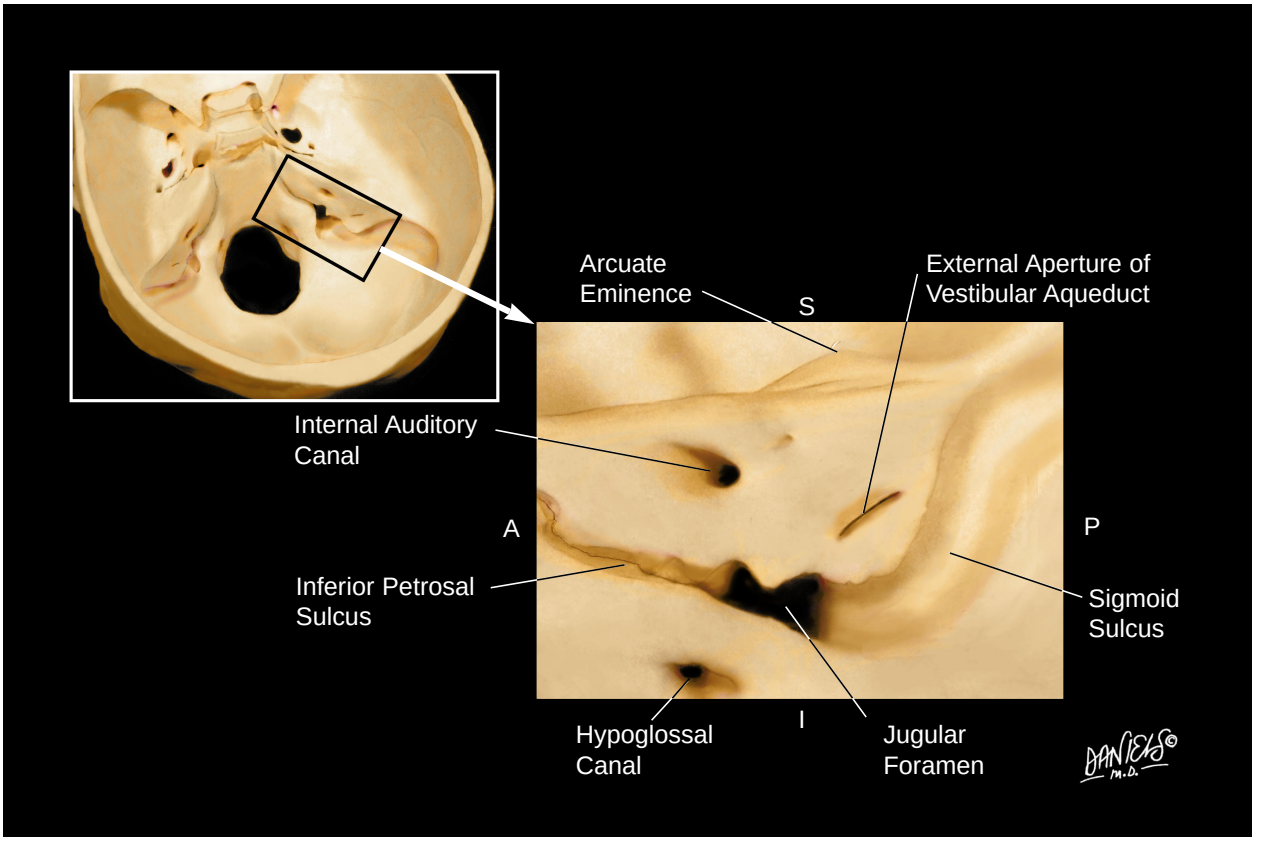

Fig 1. Anatomic landmarks on posterior surface of right petrous bone, viewed through posterior cranial fossa. *A* indicates anteromedial; *P*, posterolateral; *S*, superior; and *I*, inferior. The external aperture of the vestibular aqueduct, through which the endolymphatic sac exits the otic capsule, is a thin slit on the posterior surface of the petrous bone, inferolateral to the internal auditory canal and superior to the sigmoid sulcus. The location of this aperture is designated on subsequent drawings (Figs 2–3) for reference (modified from Donaldson et al [8]).

MR techniques, even though its internal architecture might not be resolved (11, 18) (Figs 5 and 6).

In lower animals, and in human fetuses and newborns of up to 1 year of age, the ES consists of a single lumen (19). In the human ES, beginning at about 1 year of age, tubularity develops rapidly and reaches adult complexity by 3 or 4 years of age (19). Oriented primarily longitudinally, the tubules of the ES are more complex in its proximal and middle portions, and more confluent distally (9). The middle portion of the ES, originally termed the "rugose" portion (pars rugosa) (20), is now called the *tubular* portion (pars canalicularis) by recent investigators, to describe its complex tubular pattern more accurately (5, 10) (Fig 4). The epithelial cells of the ED and ES can be flattened, cuboidal, or cylindrical (6, 9). The well-vascularized periductal and perisaccular supportive tissue is loose (21) until it gradually condenses as the distal sac merges with the dura (13) (Fig 4). The ED and ES contain only small amounts of endolymph (6, 9, 22), and are *not* surrounded by a perilymphatic space. Furthermore, the stroma of the ED and ES is more voluminous than their endolymph-filled lumen (6, 9) (Fig 4). In contrast, the remaining portions of the membranous labyrinth are smooth-walled channels, filled with larger amounts of endolymph, lying along ducts of even greater amounts of perilymph, and surrounded by little stromal tissue. Thus, the T1 and T2 of the ES are shorter than those of the remaining labyrinthine structures (23). Compared with the content of the remaining labyrinth, the content of the VA has a higher signal intensity on more T1-weighted images, and a lower signal intensity on T2-weighted or free precession images (Figs 5 and 6).

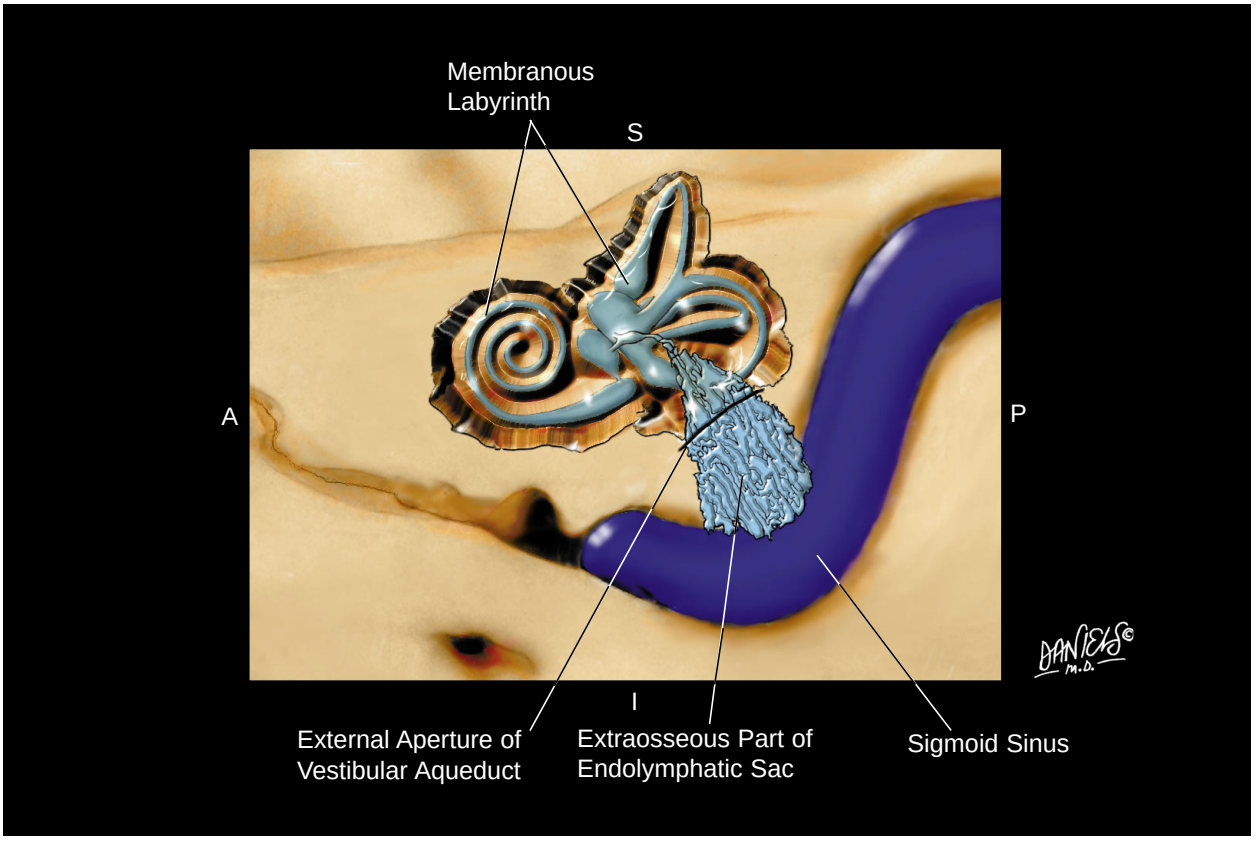

Fig 2. Cutaway view of petrous bone from Figure 1 shows the membranous labyrinth and the relationship of the endolymphatic duct and sac to the external aperture of the vestibular aqueduct and the sigmoid sinus. *A* indicates anteromedial; *P*, posterolateral; *S*, superior; and *I*, inferior. The osseous labyrinth and the perilymphatic ducts adjacent to the membranous labyrinth in the osseous labyrinth are not depicted. Note that proximal to the external aperture, the endolymphatic sac is intraosseous, lying within the vestibular aqueduct, and that distal to the external aperture, the sac is extraosseous. The distal sac often overlies the sigmoid sinus to a variable degree (modified from Ferner [2], Netter and Colacino [3], Williams [4], Schuknecht [7], and Donaldson et al [8]).

The main arterial supply of the ED and ES appears to be the occipital artery (24). The paravestibular canaliculus, or accessary canal of the VA, is an often duplicated, diminutive bony canal that carries a vein from the vestibule, parallel to the VA (6, 16). Venous blood from the sac drains into this vein near the external aperture of the VA, as well as through venules directly into the sigmoid sinus (25). Studies suggest that the ED and ES perform both absorptive and secretory (7, 22, 26, 27), as well as phagocytic (28) and immunodefensive, functions (29).

Because of the steep angulation of the long axis of the ES, at approximately 70 degrees from the infraorbital–meatal plane (30), seeing the ES on transverse images requires multiple contiguous sections (Fig 5). Sagittal images show a larger portion of the ES on a single section than do transverse images (11, 31), and demonstrate the relationship of the ES to the operculum, the dura, and the sigmoid sinus to better advantage (Fig 6A). However, in addition to the steep inclination of the length of the ES, the width of the ES lies nearly parallel to the posterior petrous surface, at an angle of about 45° from the sagittal plane of the head. Thus, seeing the entire ES on a single section requires double oblique reformation, 70° from the infraorbital–meatal plane and 45° from the sagittal (11, 31) (Fig 6B).

The ES has long been recognized for its key role in the pathogenesis of labyrinthine hydrops, which manifests clinically as Meniere disease (32), a common malady that is difficult to diagnose and treat. The symptoms of Meniere disease, which include episodic vertigo, fluctuating hearing loss, and tinnitus or aural fullness, are

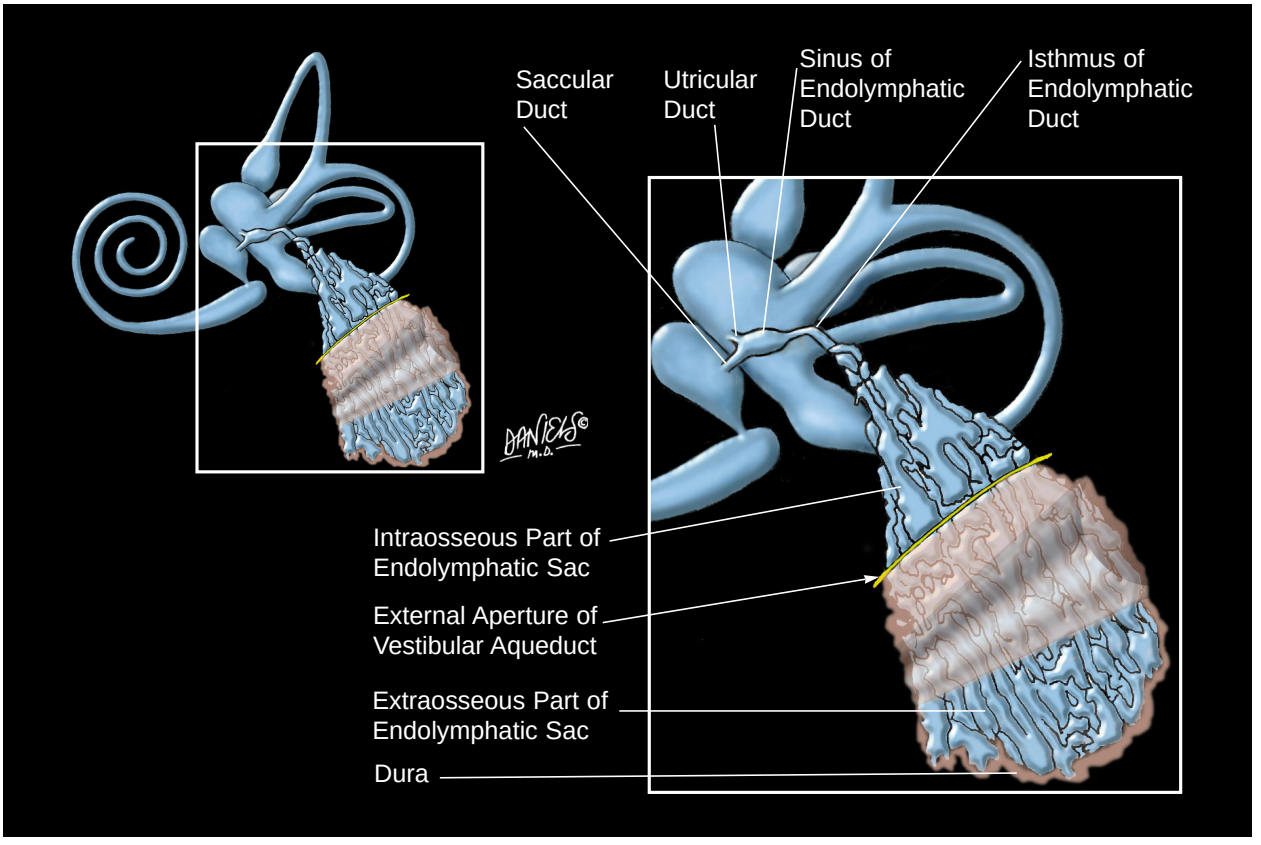

Fig 3. Membranous labyrinth (small drawing) and magnified view of endolymphatic duct and sac. The superficial layer of dura over the distal third of the extraosseous portion of the sac is reflected upward to expose the tubular architecture of the sac. The utricle is connected to the semicircular ducts, and the saccule by way of the ductus reunions, to the cochlear duct. The magnified view shows the endolymphatic duct's three parts, from anterior to posterior: (*a*) the sinus, which lies in the vestibule, (*b*) a tapered intermediate portion in the proximal vestibular aqueduct, and (*c*) the isthmus, its narrowest point, which connects with the endolymphatic sac. Some variability in the tubular pattern of the sac can occur. Under microscopy, the tubules in the distal third of the sac can be fewer and wider than shown and might not cross connect (modified from Ferner [2], Netter and Colacino [3], Williams [4], Schuknecht [7], and Donaldson et al [8]).

characteristic but nonspecific (33). Audiometric findings are of only supplementary value. With no specific test yet available, the diagnosis of Meniere disease is often imprecise. The efficacy of treatment, medical and surgical (34, 35), is sometimes difficult to evaluate because of the fluctuating natural course of the disease.

The osseous VA has been extensively studied with pleuridirectional tomography (17, 36–38) and CT (38–41) for its role in Meniere disease. Variations of the VA range from short tubular to well-developed fan-shaped structures (42). Narrower and shorter VAs (18) and smaller external apertures of the VA (43) are statistically correlated with Meniere disease, but the overlap between normal and diseased ears is too wide for this differentiation to be clinically useful.

Preliminary MR studies suggest that patients with Meniere disease often have a small or invisible ES (18, 23). Lack of visibility might correlate with the clinical course of the disease (44). In addition, enhancement after administration of contrast material might be seen in inflammation of the ED/ES (45). Nevertheless, relatively little normative MR data on the ES have been established. Furthermore, MR is still far from capable of showing Reisner's membrane or directly demonstrating endolymphatic hydrops.

The large vestibular aqueduct (wider than 1.5 mm in midsagittal diameter) is the most common congenital inner ear anomaly detectable with CT (46–48). Unlike normal ESs, endolymph-filled large ESs protruding from the large VA are readily shown with MR (49), especially on T2-weighted images (50). In fact, very

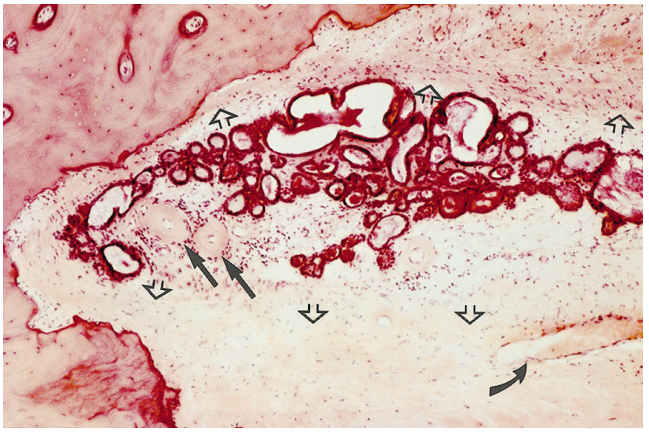

Fig 4. Photomicrograph of endolymphatic sac, transverse section in region of external aperture of vestibular aqueduct (hematoxylin-eosin, magnification ×63). The petrous bone is on top and the left. Note the large number of longitudinally oriented, cuboidal epithelium-lined tubules cut in cross sections, containing endolymph of light and dark staining properties. Several arterioles (two marked with *arrows*) and venules (one marked with *curved arrow*) lie in the abundant loosely areolar stroma, which merges gradually and indistinctly with the dense fibrous overlying and underlying dura at approximately the position of the open arrows. Towards the distal end of the sac not shown on this section, the tubules coalesce and become wider and fewer (courtesy of House Ear Institute, Los Angeles, Calif).

large ESs can be recognized even on standard CT (51). However, MR imaging delineates both the intraosseous and extraosseous volumes of the ES more accurately. Furthermore, proton density– and T1-weighted MR images can help to evaluate the sac content (52).

Papillary cystadenomatous tumors can arise from the ES, and can occur bilaterally in von Hippel-Lindau disease (53, 54). They appear as retrolabyrinthine destructive masses of varying sizes (55–57). Characteristically, they show intratumoral bone spicules on CT, foci of heterogeneous intensities on MR, usually including precontrast hyperintensities on T1-weighted images, and hypervascularity on angiography (58).

Much more of the normal and pathologic anatomy and physiology of the ED and ES remains to be learned. A thorough understanding of the anatomy of the ED and ES and their relationship to the VA, the dura, the sigmoid sinus, and the remainder of the membranous labyrinth, coupled with proper use of the anatomic terms, will facilitate our interpretation of the MR images of the ES.

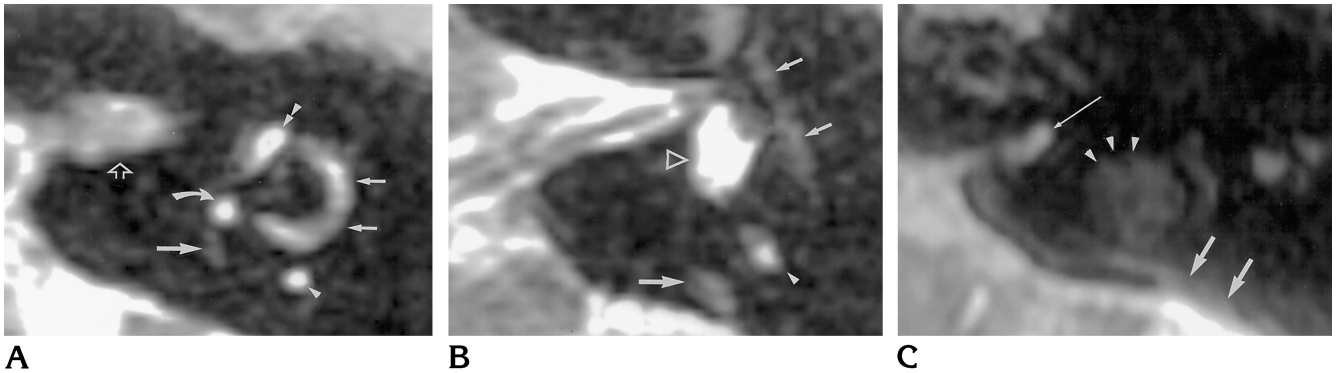

Fig 5. MR images of normal left ES. Steady-state gradient-echo sequence (23), 0.5-mm sections in transverse plane. *A*, *B*, and *C* are representative sections in order from superior to inferior.

A, At the level of the lateral semicircular canal (*small arrows*), this section transects the proximal intraosseous ES (*large arrow*) as it descends immediately posterior to the common crus (*curved arrow*). The very thin ED just medial to the common crus is not resolved. Other structures are the posterior semicircular canal (*arrowhead*), the superior semicircular canal (*double arrowhead*), and the internal auditory canal (*open arrow*).

B, At the level of the vestibule (*open arrowhead*), this section shows a segment of the distal intraosseous ES (*large arrow*). Other structures are the posterior semicircular canal (*arrowhead*) and the tympanic facial nerve canal (*small arrows*).

C, At the level inferior to the otic labyrinth, this section shows the fovea (*arrows*) immediately inferior to the external aperture of the vestibular aqueduct, on which rests the extraosseous ES, inseparable from dural layers. Other structures are the jugular bulb (*arrowheads*) and the cochlear aqueduct (*thin arrow*). Note that the *normal* vestibular aqueduct content is of lower signal intensity than are other labyrinthine structures and cerebrospinal fluid.

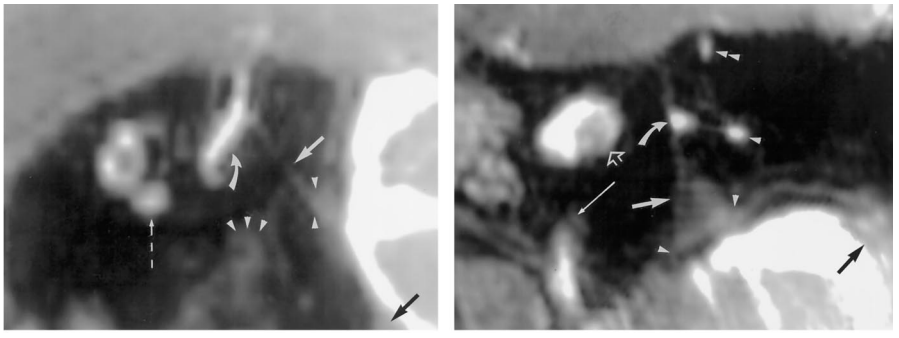

A B

Fig 6. MR images of normal left ES, steady-state gradient-echo sequence, 1-mm sections; *A* is sagittal and *B* double oblique. The intraosseous ES (*arrow*) is clearly seen between the common crus (*curved arrow*) and the external aperture (*between two arrowheads*). On *A*, the ES appears as a thin straight linear structure. On *B*, it appears as a narrow-based triangle that widens as it descends from medial to the common crus towards the posterior surface of the petrous bone. The ED is not seen on A or B. Other structures are the sigmoid sinus (*black arrow*), jugular bulb (*three arrowheads*), cochlea (*interrupted arrow*), posterior semicircular canal (*arrowhead*), superior semicircular canal (*double arrowhead*), internal auditory canal (*open arrow*), and cochlear aqueduct (*thin arrow*). The operculum covering the ES from the posterior fossa is unmarked. Note again that the *normal* vestibular aqueduct content is lower in signal intensity than that of other labyrinthine structures and cerebrospinal fluid.

References

1. Danckwardt-Lilliestrom N, Rask-Andersen H, Linthicum FH, House WF. A technique to obtain and process surgical specimens of the human vestibular aqueduct for histopathological studies of the endolymphatic duct and sac. *ORL J Otorhinolaryngol Relat Spec* 1992;54:215–219
2. Ferner H, ed. *Eduard Pernkopf: Atlas of topical and applied human anatomy*, Vol 1: *Head and Neck*. 2nd ed. Baltimore, Md: Urban & Schwarzenberg; 1980;1:161–162
3. Netter FH, Colacino S, eds. *Atlas of Human Anatomy*. Summit, NJ: Ciba Geigy Corp; 1989, plates 90–91
4. Williams PL, ed. *Gray's Anatomy*. 38th ed. New York, NY: Churchill Livingstone; 1995;1378
5. Antunez J-CM, Galey FR, Linthicum FH, McCann GD. Computer-aided and graphic reconstruction of the human endolymphatic duct and sac: a method for comparing Meniere's and non-Meniere's disease cases. *Ann Otol Rhinol Laryngol* 1980;89(suppl 76):23–32
6. Friberg U, Rask-Andersen H, Bagger-Sjöbäck D. Human endolymphatic duct: an ultrastructure study. *Arch Otolaryngol* 1984;110:421–428
7. Schuknecht HF. *Pathology of the Ear*. Philadelphia, Pa: Lea & Febiger; 1993:45–47, 50–51, 62, 64, 101
8. Donaldson JA, Duckert LG, Lambert PM, Ruble EW. *Anson-Donaldson Surgical Anatomy of the Temporal Bone*. 4th ed. New York, NY: Raven; 1992:96, 226, 314–327, 334–442
9. Bagger-Sjöbäck D, Jansson B, Friberg U, Rask-Andersen H. Three-dimensional anatomy of the human endolymphatic sac. *Arch Otolaryngol Head Neck Surg* 1990;116:345–349
10. Hebbar GK, Rask-Andersen H, Linthicum FH Jr. Three-dimensional analysis of 61 human endolymphatic ducts and sacs in ears with and without Meniere's disease. *Ann Otol Rhinol Laryngol* 1991;100:219–225
11. Oehler MC, Chakeres DW, Schmalbrock P. Reformatted planar ''Christmas tree'' MR appearance of the endolymphatic sac. *AJNR Am J Neuroradiol* 1995;16:1525–1528
12. Lang J. *Clinical Anatomy of the Posterior Cranial Fossa and Its Foramina*. New York, NY: Thieme; 1991:4–6
13. Friberg U, Jansson, Rask-Andersen H, Bagger-Sjöbäck D. Variations in surgical anatomy of the endolymphatic sac. *Arch Otolaryngol Head Neck Surg* 1988;114:389–394
14. Schuknecht HF, Gulya AJ. *Anatomy of the Temporal Bone with Surgical Implications*. Philadelphia, Pa: Lea & Febiger; 1986:145–156
15. Ogura Y, Clemis JD. A study of the gross anatomy of the human vestibular aqueduct. *Ann Otol Rhinol Laryngol* 1971;80:813–825
16. Wilbrand HF, Rask-Andersen H, Gilstring D. The vestibular aqueduct and the paravestibular canal: an anatomic and radiologic investigation. Acta Radiol 1974;15:337–355
17. Stahle J, Wilbrand HF, Rask-Andersen H. Temporal bone characteristics in Meniere's disease. *Ann N Y Acad Sci* 1981;374: 794–807
18. Tanioka H, Zusho H, Machida T, Sasaki Y, Shirakawa T. High-resolution MR imaging of the inner ear: findings in Meniere's disease. *Eur J Radiol* 1992;15:83–88
19. Ng M, Linthicum FH Jr. Morphology of the developing endolymphatic sac. *Laryngoscope* (in press)
20. Bast TH, Anson BJ. The temporal bone and the ear. Springfield, Ill: Charles C Thomas; 1949:43–64
21. Rask-Andersen H, Friberg U, Bagger-Sjöbäck D. The ultrastructure of the human endolymphatic duct. *Acta Otolaryngol* 1984; 406(s):61–66
22. Wackym PA, Friberg U, Bagger-Sjöbäck D, Linthicum FH Jr, Friedmann I, Rask-Andersen H. Human endolymphatic sac: possible mechanisms of pressure regulation. *J Laryngol Otol* 1987; 101:768–779
23. Schmalbrock P, Dailiana T, Chakeres DW, et al. Submillimeter-resolution MR of the endolymphatic sac in healthy subjects and patients with Meniere disease. *AJNR Am J Neuroradiol* 1996;17: 1707–1716
24. Gadre AK, Fayad JN, O'Leary MJ, Zakhary R, Linthicum FH Jr. Arterial supply of the human endolymphatic duct and sac. *Otolaryngol Head Neck Surg* 1993;108:141–148
25. Gussen R. Endolymphatic hydrops with absence of vein in paravestibular canaliculus. *Ann Otol* 1980;89:157–161
26. Yeo SW, Gottschlich S, Harris JP, Keithley EM. Antigen diffusion from the perilymphatic space of the cochlea. *Laryngoscope* 1995; 105:623–628
27. Rask-Andersen H, Danckwardt-Lilliestrom N, Linthicum FH, House WF. Ultrastructural evidence of a merocrine secretion in the human endolymphatic sac. *Ann Otol Rhinol Laryngol* 1991; 100:148–156

28. Fukuzawa K, Sakagami M, Matsunaga T, Fujita H. Endocytotic activity of the free floating cells and epithelial cells in the endolymphatic sac: an electron microscopic study. *Anat Rec* 1991; 230:425–433
29. Wackym PA, Friberg U, Linthicum FH Jr, et al. Human endolymphatic sac: morphologic evidence of immunologic function. *Ann Otol Rhinol Laryngol* 1987;96:276–282
30. Chakeres DW, Spiegel PK. A systematic method for comprehensive evaluation of the temporal bone by computed tomography. *Radiology* 1983;146:97–106
31. Chakeres DW, Oehler M, Schmalbrock P, Slone W. Temporal bone imaging. In: Som PM, Curtin HD, eds. *Head and Neck Imaging*. 3rd ed. St Louis, Mo: Mosby; 1996:1328, 1339, 1346
32. Wackym PA, Linthicum FH Jr, Ward PH, House WF, Micevych PE, Bagger-Sjöbäck D. Re-evaluation of the role of the human endolymphatic sac in Meniere's disease. *Otolaryngol Head Neck Surg* 1990;102:732–744
33. Committee on Hearing and Equilibrium guidelines for the diagnosis and evaluation of therapy in Meniere's disease. *Otolaryngol Head Neck Surg* 1995;113:181–185
34. Lassen LF, Hirsch BE, Kamerer DB. Use of nimodipine in the medical treatment of Meniere's disease: clinical experience. *Am J Otol* 1996;17:577–580
35. Shea JJ Jr. Classification of Meniere's disease. *Am J Otol* 1993; 14:224–229
36. Clemis JD, Valvassori GE. Recent radiographic and clinical observations on the vestibular aqueduct. *Otolaryngol Clin North Am* 1968;1:339–346
37. Stahle J, Wilbrand H. The vestibular aqueduct in patients with Meniere's disease: a tomographic and clinical investigation. *Acta Otolaryngol* 1974;78:36–48
38. Dreisbach J, Seibert C, Arenberg IK. Patency and visibility of the vestibular aqueduct in Meniere's disease. *Otolaryngol Clin North Am* 1983;16:103–113
39. Valvassori GE, Dobben GD. Multidirectional and computerized tomography of the vestibular aqueduct in Meniere's disease. *Ann Otol Rhinol Layrngol* 1984;93:547–550
40. Nidecker A, Pfaltz CR, Matéfi L, Benz UF. Computer tomographic findings in Meniere's disease. *ORL J Otorhinolaryngol Relat Spec* 1985;47:66–75
41. De Groot JAM, Huizing EH. Computed tomography investigation of the vestibular aqueduct in Meniere's disease. *Acta Otolaryngol* 1986;suppl 434:96–135
42. Sando I, Ikeda M. The vestibular aqueduct in patients with Meniere's disease: a temporal bone histopathological investigation. *Acta Otolaryngol* 1984;97:558–570
43. Yamamoto E, Mizukami C, Isono M, Ohmura M, Hirono Y. Observation of the external aperture of the vestibular aqueduct using three-dimensional surface reconstruction imaging. *Laryngoscope* 1991;101:480–483
44. Tanioka H, Kaga K, Zusho H, Araki T, Sasaki Y. MR of the endolymphatic duct and sac: findings in Meniere disease. *AJNR Am J Neuroradiol* 1997;18:45–51
45. Fitzgerald DC, Mark AS. Endolymphatic duct/sac enhancement on gadolinium magnetic resonance imaging of the inner ear: preliminary observations and case reports. *Am J Otol* 1996;17: 603–606
46. Valvassori GE, Clemis JD. The large vestibular aqueduct syndrome. *Laryngoscope* 1978;88:723–728
47. Mafee MF, Charletta D, Kumar A, Belmont H. Large vestibular aqueduct and congenital sensorineural hearing loss. *AJNR Am J Neuroradiol* 1992;13:805–819
48. Urman SM, Talbot JM. Otic capsule dysplasia: clinical and CT findings. *Radiographics* 1990;10:823–838
49. Hirsch BE, Weissman JL, Curtin HD, Kamerer DB. Magnetic resonance imaging of the large vestibular aqueduct. *Arch Otolargol Head Neck Surg* 1992;118:1124–1127
50. Harnsberger HR, Dahlen RT, Shelton C, Gray SD, Parkin JL. Advanced techniques in magnetic resonance imaging in the evaluation of the large endolymphatic duct and sac syndrome. *Laryngoscope* 1995;105:1037–1042
51. Levenson MJ, Parisier SC, Jacobs M, Edelstein DR. The large vestibular aqueduct syndrome in children. *Arch Otolaryngol Head Neck Surg* 1989;115:54–58
52. Okamoto K, Ito J, Furusawa T, Sakai K, Tokiguchi S. Large vestibular aqueduct syndrome with high CT density and high MR signal intensity. *AJNR Am J Neuroradiol* 1997;18:482–484
53. Megerian CA, McKenna MJ, Nuss RC, et al. Endolymphatic sac tumors: histopatholic confirmation, clinical characterization, and implication in von Hippel-Lindau disease. *Laryngoscope* 1995; 105:801–808
54. Kempermann G, Neumann HPH, Scheremet R, et al. Deafness due to bilateral endolymphatic sac tumors in a case of von Hippel-Lindau syndrome. *J Neurol Neurosurg Psychiatry* 1996;16:318–320
55. Lo WWM, Applegate LJ, Carberry JN, et al. Endolymphatic sac tumors: radiologic diagnosis. *Radiology* 1993;189:199–204
56. Meyer JR, Gebarski SS, Blaivas M. Cerebellopontine angle invasive papillary cystadenoma of endolymphatic sac origin with temporal bone involvement. *AJNR Am J Neuroradiol* 1993;14:1319–1321
57. Ho VT, Rao VM, Doan HT, Mikalian DO. Low-grade adenocarcinoma of probable endolymphatic sac origin: CT and MR appearance. *AJNR Am J Neuroradiol* 1996;17:168–170
58. Mukherji SK, Castillo M. Adenocarcinoma of the endolymphatic sac: imaging features and preoperative embolization. *Neuroradiology* 1996;38:179–180